Hassan Ali Khan, 2026, 14:4
ISSN (Online): 2348-4098
ISSN (Print): 2395-4752

International Journal of Science, Engineering and Technology
An Open Access Journal

Extraction of the Kinetic Freeze-Out Temperature by an alternative Method: A Fokker–Planck Analysis

Hassan Ali Khan[1], Hadiqa Qadir[2]

[1]Hubei Key Laboratory of Energy Storage and Power Battery, School of Optoelectronic Engineering, School of New Energy, Hubei University of Automotive Technology, Shiyan 442002, China

[2]Department of Physics, Abdul Wali Khan University Mardan, Mardan 23200, Pakistan

Abstract- The extracted kinetic freezeout temperature reflects the thermal conditions of the system at the final stage of elastic interactions, and is typically obtained through simultaneous fits of transverse momentum spectra using blast-wave-type models that also yield the average radial flow velocity. In this study, we extract the kinetic freeze-out temperature, Tkin, from the transverse momentum spectra of identified negativley charged hadrons π−, K− and p− produced in Au–Au collisions across the RHIC Beam Energy Scan, spanning √sNN = 7.7 to 200 GeV. Our analysis builds upon effective temperatures obtained in our previous work, from which we isolate the kinetic decoupling temperature by applying a linear fit, Teff = m m0 + Tkin, to the particle mass dependence of the effective temperatures. We present two independent sets of fitting results, which show consistent qualitative behaviors and provide robust estimates of the freeze-out parameters. Our extracted values of Tkin reveal two clear and systematic trends. For any fixed collision energy, the freeze-out temperature decreases monotonically as we move from central to peripheral collisions, reflecting the diminishing system size, lower energy density, and reduced rescattering in the later stages of the fireball evolution. For a fixed centrality bin, the temperature rises with increasing beam energy, but the rise is not uniform: a steep increase at low energies is followed by a plateau around 19.6–39 GeV, which then gives way to a renewed rise at the highest RHIC energies. This non-monotonic behaviour is interpreted as evidence for a change in the underlying degrees of freedom, consistent with the system transitioning from a baryon-rich hadronic phase through a possible crossover region and into a parton-dominated phase at the highest energies. The results demonstrate that the kinetic freeze-out temperature is a sensitive probe of the system size, initial energy density, and the stiffness of the equation of state. Our findings provide important constraints for hydrodynamic models and highlight the utility of the Fokker–Planck approach in extracting freeze-out parameters from experimental data.

Keywords: kinetic freezeout temperature; effective temperature; hydrodynamic simulations; Fokker Planck.

I. INTRODUCTION

The kinetic freezeout temperature is the point at which elastic collisions among hadrons in the expanding fireball cease, freezing their momentum distributions for detection, Tkin[1, 2, 3, 4, 5, 6, 7], starts with defining exactly what this parameter precisely characterizes the physical state of the system during the terminal stages of ultra-relativistic heavy-ion collisions. It corresponds to the specific epoch in the fireball's expansion at which the mean free path of a hadron defined as the average distance traversed between successive scatterings becomes comparable to the characteristic size of the emitting system. Beyond this point, the frequency of elastic interactions diminishes substantially, such that hadrons can no longer sustain effective momentum exchange with the surrounding medium. Consequently, the particles undergo free streaming toward the detector, preserving the momentum and velocity distributions established at the instant of final thermal contact.

The kinetic freezeout temperature,therefore constitutes a direct thermodynamic signature of this decoupling stage, encapsulating the combined contributions of random thermal motion and collective radial expansion at the conclusion of the system's dynamical evolution. Once the fireball reaches this point, elastic collisions like π + π π + π are no longer frequent enough to sustain local thermal equilibrium. The moment the system crosses this threshold, the hadrons effectively decouple from the collective flow and begin to free-stream toward the detectors. Consequently, the momentum spectra we eventually measure are essentially snapshots frozen in time, unaltered by any further interactions. To fully appreciate this, one has to separate Tkin from the chemical freezeout temperature, Tch [8, 9, 10, 11], which happens much earlier at around 150 160 MeV. At chemical freezeout, inelastic processes cease to operate, thereby fixing the final-state particle yields and their relative abundances. The system, however, does not decouple instantaneously; rather, it persists as a dense hadronic medium in which elastic scatterings continue to redistribute momentum and energy among the constituent particles.

This intermediate stage, situated between chemical and kinetic freezeout, is characterized by the conservation of particle identities alongside ongoing modification of their kinematic distributions through residual hadronic rescattering. This intermediate stage, situated between chemical and kinetic freezeout, is characterized by the conservation of particle identities alongside ongoing modification of their kinematic distributions through residual hadronic rescattering. Only later, when the expanding fireball cools adiabatically down to the 90 − 120 MeV range, these elastic processes become rare enough to be considered practically absent. This makes Tkin the final thermodynamic snapshot we have of the strongly interacting medium before it turns into a gas of non-interacting particles.

This is very important that Why does this particular temperature attract so much attention? For one, it offers a direct window into the transport properties [12, 13, ?, 14, 15] of the created matter, especially the ratio of shear viscosity to entropy density, η/s [13, 16]. If the system behaves as a near-perfect fluid characterized by very low viscosity, it undergoes smooth expansion with minimal internal friction. Such a medium preserves its thermal distribution for a comparatively extended duration and consequently cools to a lower kinetic freezeout temperature prior to decoupling. Conversely, a highly viscous medium dissipates its internal pressure gradients more rapidly, causing elastic collisions to cease at an earlier stage, which in turn results in a noticeably higher kinetic freezeout temperature, Tkin.

Thus, by measuring this temperature, we impose stringent constraints on the microscopic dissipative processes that operate from the quark-gluon plasma phase all the way through the late hadronic stage. Besides, Tkin plays in disentangling the underlying dynamics of the expanding fireball. The final observed spectra are a convolution of two effects: random thermal motion of the particles and the collective radial outflow driven by the system's internal pressure. Without a handle on the decoupling temperature, we would struggle to separate these two contributions.

Knowing Tkin allows us to isolate the collective flow component, which in turn enables a quantitative investigation of the hadronic equation of state, specifically how effectively the internal energy gets converted into bulk directed expansion. It should be noted that the combination of kinetic freezeout temperature and collective radial flow is often known as the effective temperature (Teff) [17, 18, 19, 20]. Besides, the three discussed temperatures, the initial temperature [43, 22, 23, 24] is also important which occurs in the initial stages of collisions. These temperature follow a general trend Ti > Tch > Teff > Tkin [25, 26, 27, 28]. Besides, Tkin plays a crucial role in disentangling the underlying dynamics of the expanding reball.

The nal observed spectra are a convolution of two e ects: random thermal motion of the particles and the collective radial out ow driven by the system's internal pressure. Without a handle on the decoupling temperature, we would struggle to separate these two contributions. Knowing Tkin allows us to isolate the collective ow component, which in turn enables a quantitative investigation of the hadronic equation of state, speci cally how e ectively the internal energy gets converted into bulk directed expansion.

On the theoretical side, this temperature serves as a pivotal anchor for hydrodynamic simulations. These models run a fluid-dynamical evolution until some chosen switching temperature, after which they hand over the description to a microscopic hadronic cascade to handle the late, dilute phase. If this artificially chosen matching point deviates from the actual experimentally extracted Tkin, the simulation's predicted momentum distributions will inevitably fail to match the real data. Therefore, this observable effectively tells theorists exactly when the fluid picture breaks down and when one must start treating the system as a free-streaming gas.

One of the more subtle and fascinating points is that Tkin is not strictly a universal global value; it shows a clear dependence on the particle species under consideration. Heavier hadrons, such as protons, have smaller elastic cross-sections and therefore tend to decouple earlier when the fireball is still relatively hot, say around 115 MeV. In contrast, light pions have larger interaction probabilities and continue to scatter for a longer period, eventually freezing out at a lower temperature, closer to 95 MeV.

This differential decoupling provides clear experimental evidence that the late hadronic phase is not a passive gas; instead, it involves ongoing momentum exchanges that selectively affect different particles based on their interaction strengths. Finally, consider the implications for anisotropic flow harmonics [29, 30, 31], such as the elliptic flow v2 and triangular flow v3 [32, 33]. These collective anisotropies are primarily generated in the early quark-gluon plasma phase due to the initial spatial asymmetries of the collision zone.

However, the subsequent hadronic phase can still alter these signals through residual scatterings; depending on the conditions, it might amplify them or smear them out. By pinning down the exact decoupling temperature, physicists can quantify how much of the final observed flow originated from the late hadronic rescattering stage as opposed to the earlier partonic stage. This completes the comprehensive picture of the fireball's evolution, from the hottest and densest medium ever created in the laboratory to the free-streaming particles that ultimately leave their signatures in our detectors.

Table 1: Values of free parameters (T1, T2) and χ2/dof corresponding to the fits (set 1).

Collisions	Centrality (%)	Slope	Intercept	χ^2/dof
	0–5	0.260 ± 0.007	0.220 ± 0.006	60.5
	5–10	0.258 ± 0.006	0.215 ± 0.004	253.2
	10–20	0.257 ± 0.004	0.210 ± 0.003	260.9
Au–Au 7.7 GeV	20–30	0.259 ± 0.005	0.206 ± 0.002	40.6
	30–40	0.262 ± 0.003	0.200 ± 0.003	99.0
	40–50	0.264 ± 0.008	0.194 ± 0.005	55.9
	50–60	0.266 ± 0.007	0.187 ± 0.004	948.7
	60–70	0.268 ± 0.003	0.181 ± 0.002	27.1
	70–80	0.270 ± 0.004	0.175 ± 0.002	39.4
	0–5	0.258 ± 0.006	0.239 ± 0.005	
	5–10	0.256 ± 0.004	0.235 ± 0.003	696.4
	10–20	0.254 ± 0.005	0.230 ± 0.002	722.7
Au–Au 11.5 GeV	20–30	0.253 ± 0.003	0.226 ± 0.004	317.2
	30–40	0.255 ± 0.002	0.220 ± 0.002	315.4
	40–50	0.260 ± 0.003	0.212 ± 0.002	181.8
	50–60	0.257 ± 0.004	0.208 ± 0.003	328.9
	60–70	0.261 ± 0.005	0.202 ± 0.004	318.5
	70–80	0.263 ± 0.006	0.196 ± 0.003	716.3
	0–5	0.264 ± 0.004	0.262 ± 0.005	671.0
	5–10	0.266 ± 0.005	0.257 ± 0.003	288.3
	10–20	0.268 ± 0.006	0.251 ± 0.004	162.1
20–30		0.267 ± 0.005	0.246 ± 0.003	661.7
Au–Au 14.5 GeV	30–40	0.263 ± 0.004	0.244 ± 0.005	101.2
	40–50	0.260 ± 0.007	0.240 ± 0.004	287.9
	50–60	0.258 ± 0.005	0.235 ± 0.003	670.5
	60–70	0.261 ± 0.004	0.230 ± 0.005	633.7
	70–80	0.265 ± 0.006	0.222 ± 0.004	50.05

continued on next page

Table 1 – continued

Collisions	Centrality (%)	Slope	Intercept	χ^2/dof
	0–5	0.266 ± 0.007	0.292 ± 0.005	233.3
	5–10	0.264 ± 0.005	0.287 ± 0.003	138.5
	10–20	0.261 ± 0.006	0.283 ± 0.004	559.0
	20–30	0.259 ± 0.004	0.280 ± 0.002	536.6
Au–Au 19.6 GeV	30–40	0.256 ± 0.004	0.277 ± 0.003	49.4
	40–50	0.263 ± 0.003	0.270 ± 0.004	57.0
	50–60	0.268 ± 0.006	0.261 ± 0.005	525.8
	60–70	0.267 ± 0.005	0.256 ± 0.006	539.5
	70–80	0.265 ± 0.007	0.253 ± 0.005	57.0
	0–5	0.264 ± 0.008	0.292 ± 0.004	243.7
	5–10	0.262 ± 0.005	0.288 ± 0.003	137.1
	10–20	0.260 ± 0.006	0.285 ± 0.002	524.2
	20–30	0.261 ± 0.007	0.280 ± 0.004	535.6
Au–Au 27 GeV	30–40	0.263 ± 0.005	0.273 ± 0.003	43.9
	40–50	0.265 ± 0.006	0.267 ± 0.005	60.8
	50–60	0.270 ± 0.008	0.260 ± 0.004	526.3
	60–70	0.259 ± 0.007	0.261 ± 0.006	516.5
	70–80	0.258 ± 0.006	0.255 ± 0.005	61.7
	0–5	0.264 ± 0.006	0.292 ± 0.009	138.5
	5–10	0.262 ± 0.007	0.288 ± 0.008	547.6
	10–20	0.260 ± 0.006	0.284 ± 0.005	87.6
	20–30	0.258 ± 0.005	0.280 ± 0.004	137.2
Au–Au 39 GeV	30–40	0.259 ± 0.004	0.275 ± 0.005	134.1
	40–50	0.266 ± 0.006	0.268 ± 0.007	223.1
	50–60	0.265 ± 0.007	0.262 ± 0.006	87.0
	60–70	0.263 ± 0.005	0.258 ± 0.004	238.2
	70–80	0.261 ± 0.008	0.253 ± 0.007	46.2
	0–5	0.298 ± 0.009	0.309 ± 0.007	4.7
	5–10	0.300 ± 0.007	0.304 ± 0.006	2.8
	10–20	0.302 ± 0.006	0.298 ± 0.005	3.7
	20–30	0.305 ± 0.005	0.292 ± 0.004	1.3
Au–Au 62.4 GeV	30–40	0.304 ± 0.008	0.286 ± 0.007	21.4
	40–50	0.303 ± 0.004	0.282 ± 0.006	5.4
	50–60	0.296 ± 0.006	0.280 ± 0.004	2.5
	60–70	0.299 ± 0.005	0.275 ± 0.006	4.8
	70–80	0.295 ± 0.007	0.270 ± 0.005	30.4
	0–5	0.329 ± 0.006	0.323 ± 0.005	716.8
	5–15	0.327 ± 0.007	0.318 ± 0.004	742.1
30 GeV	15–30	0.325 ± 0.005	0.315 ± 0.006	23.6
	30–60	0.322 ± 0.008	0.310 ± 0.007	2.4
	60–90	0.323 ± 0.004	0.305 ± 0.005	4.3
	0–5	0.316 ± 0.009	0.365 ± 0.008	2.2
	5–10	0.314 ± 0.007	0.360 ± 0.005	1.5
	10–20	0.311 ± 0.008	0.355 ± 0.006	7.2
	20–30	0.308 ± 0.006	0.353 ± 0.005	6.2

Table 1 – continued

Collisio Centrality (%)	Slope	Intercept	χ^2/dof
30–40	0.306 ± 0.007	0.349 ± 0.007	3.1
40–50	0.313 ± 0.006	0.340 ± 0.006	6.6
50–60	0.309 ± 0.005	0.339 ± 0.003	1.8
60–70	0.315 ± 0.004	0.332 ± 0.005	2.3
70–80	0.305 ± 0.007	0.331 ± 0.006	15.1

II. THE METHOD AND FORMALISM

We used the fokker planck model [40] to analyze the transverse momentum spectra of the negativley charged particles π−, K− and p− to extract the freezeout parameters. Several models can be used for this purpose, for instance; the blast wave model with Boltzman Gibbs statistics [41, 42], blast wave model with Tsallis statistics [43, 44], standard distribution [45], hagedorn thermal model [46] and so on. We used fokker plank model due to less work has been done with this model. The whole methodology of fokker planck model is presented in [40] in detail. The corresponding parameters were extracted.

Generally, we have two methods in literature for the extraction of the parameters. One is the direct method and the other is indirect method. In the first method, the parameters are extracted directly from the pT spectra, and the second method the parameters are indirectly extracted from the pT spectra. For instance, if we extract the effective temperature from the pT spectra directly, as discussed earlier that effective temperature included the flow effect. So we can separate the kinetic freezeout temperature and transverse flow velocity from the effective temperature, and we can also extract the initial temperature of the emission sources from the mean transverse momentum by the string percolation method.

In the present work, we extract the kinetic freezeout temperature from the effective temperature obtained in our recent work [34]. We fit the extracted effective temperature of all the particles within each centrality bins at a specific energy by the linear fit equation which is y=xm + z where x is slope and z is the intercept, and z is regarded as the kinetic freezeout temperature.

III. RESULTS AND DISCUSSIONS

Figure 1 demonstrates the effective temperature obtained in our previous work [34] in different centrality intervals and at different energies for π−, K− and p−. The effective temperature is plotted against the rest mass of the particles, and fit it with the help of linear fit equation to extract the slopes and intercepts. The values of slopes, intercepts, and χ2 are tabulated in table 1.

Looking at figure 1, the data points represent the effective temperature obtained in our recent work [34], and the curve over these points are the results of our fit by using the linear fit equation. However, figure1 demonstrates the results for negativley charged particles. In this figure, the effective temperature is displayed on y-axis, while the rest of the particles is displayed on x-axis.

Figure 2 demonstrates the mean kinetic freezeout (Tkin) dependence of centrality and center of mass energy. The trend of symbols from up do downward shows the results of kinetic freezeout temperature with changing centrality, while from left to right the kinetic freezeout temperature is shown as function of center of mass energy. Taking the intercepts from the two fitting sets at face value, one obtains a direct experimental measure of the kinetic freeze-out temperature, Tkin. Scanning through the numbers, two exceptionally clean and physically transparent patterns emerge. The first concerns the centrality dependence for any fixed collision energy: as we move from the most central events (0 − 5%) toward the most peripheral ones (70 − 80%), the freeze-out temperature drops systematically. To give a concrete example, at sNN = 200 GeV the intercept falls from roughly 0.365 in the 0 − 5% bin to about 0.330 in the 70 − 80% bin; the same monotonic decline is observed at every energy down to 7.7 GeV, where the corresponding values decrease from approximately 0.220 to 0.175.

This behavior is naturally understood from the evolution of the expanding fireball. In central collisions, the large nuclear overlap volume and the high number of participating nucleons deposit an enormous amount of energy into a compact region, giving rise to a dense, long-lived medium where particles undergo frequent rescatterings. This prolonged thermalisation pushes the decoupling surface to a later stage, when the system is still comparatively hot. Peripheral collisions, on the other hand, produce small fireballs that expand rapidly; the particle density drops quickly, rescatterings become scarce, and the system decouples early, at a significantly lower temperature.

The second equally prominent trend emerges when we vary the beam energy for a fixed centrality bin. The freeze-out temperature rises monotonically with increasing $\sqrt{s_{NN}}$, yet the rise is not uniform. Taking the most central bin as an illustration, the intercept climbs steeply from 0.220 at 7.7 GeV to 0.292 at 19.6 GeV, then levels off into a noticeable plateau around 0.292 at 39 GeV, before resuming its upward course to 0.309 at 62.4 GeV and eventually reaching 0.365 at 200 GeV. This energy dependence can be understood as a traversal through different physical regimes of the produced matter. At the lowest energies, the system is baryon-rich and the equation of state is relatively stiff, making the temperature highly sensitive to the deposited energy and explaining the sharp initial rise.

In the intermediate region around 19-39 GeV, the medium is believed to cross over from a hadron-dominated to a parton-dominated phase; the softening of the equation of state in this crossover region naturally suppresses the temperature's response to further increases in the beam energy, giving rise to the observed plateau. At the highest RHIC energies, the system confidently enters the quark-gluon plasma phase; although strong radial flow develops and cools the expanding matter, the extreme initial temperatures are so high that the freeze-out surface is pushed to substantially larger values, as reflected in the final steep increase.

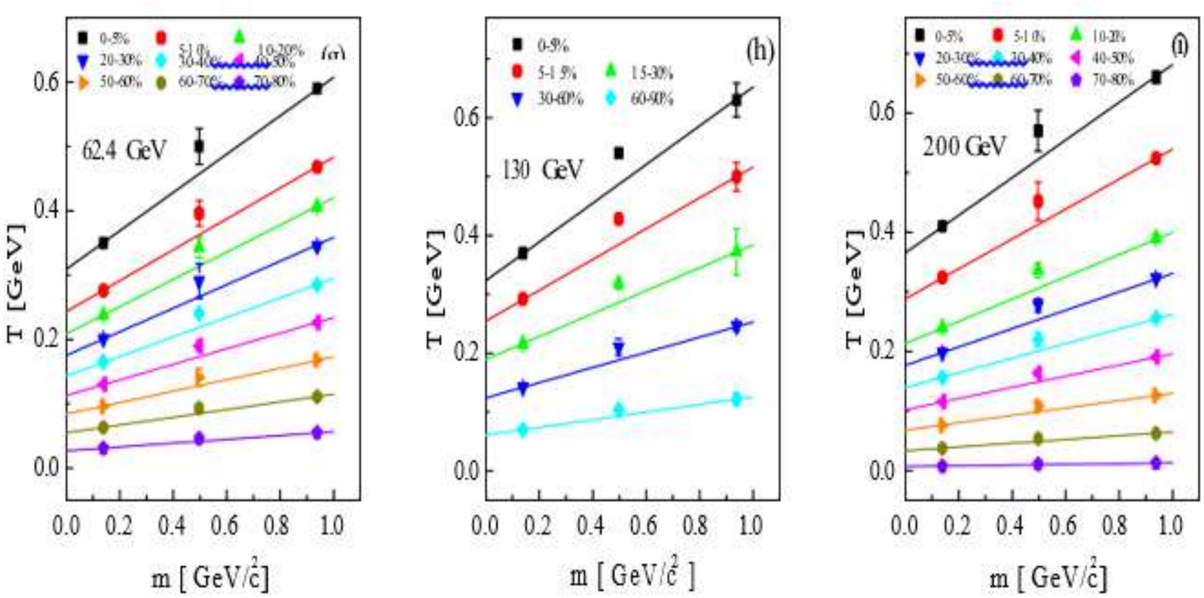

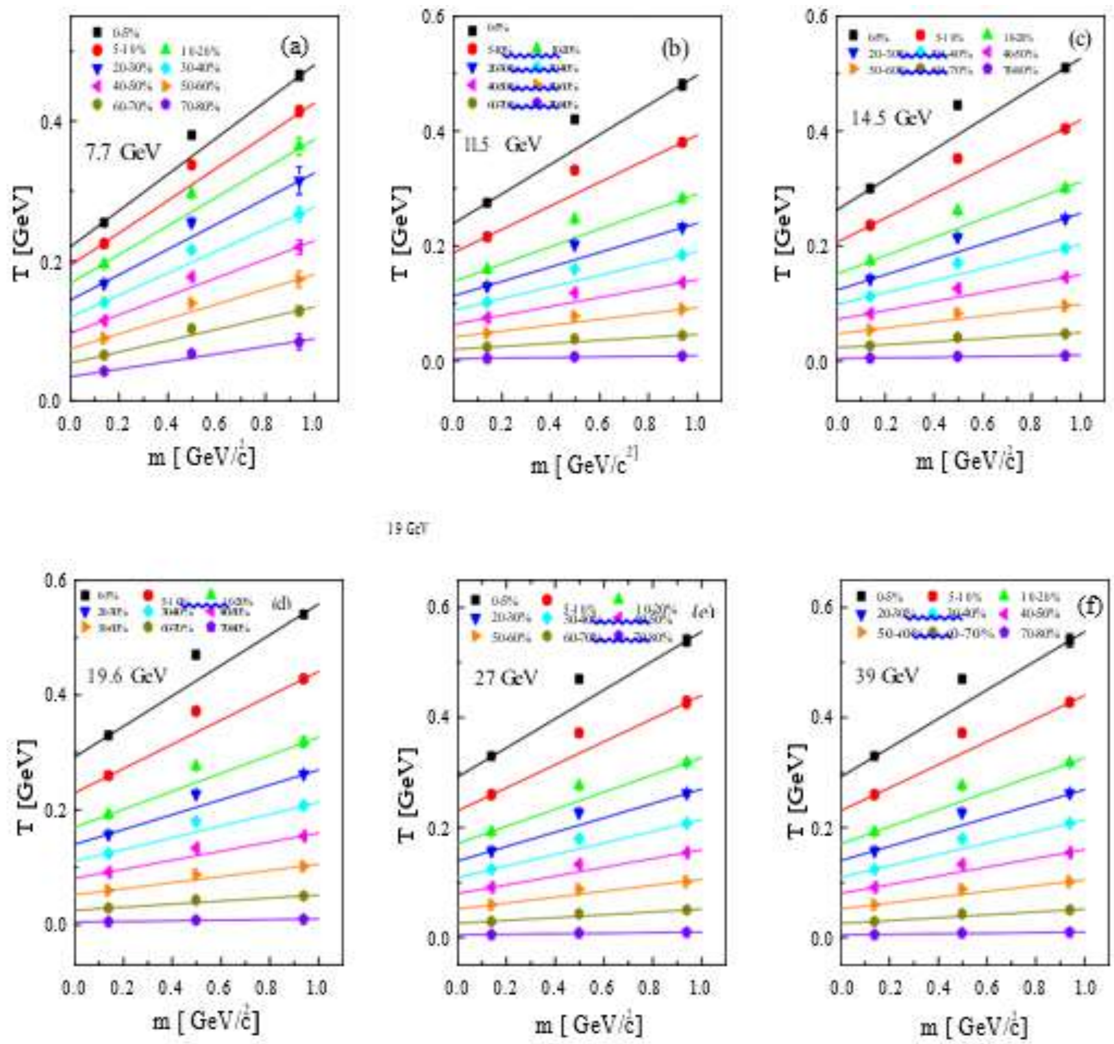

Figure 1: The effective temperature obtained in our recent work for negativley charged particles π−, K− and p− [34] are plotted against the rest mass of the particles. The data points are the values of effective temperature and the curve over them are our fit results by the linear fit equation

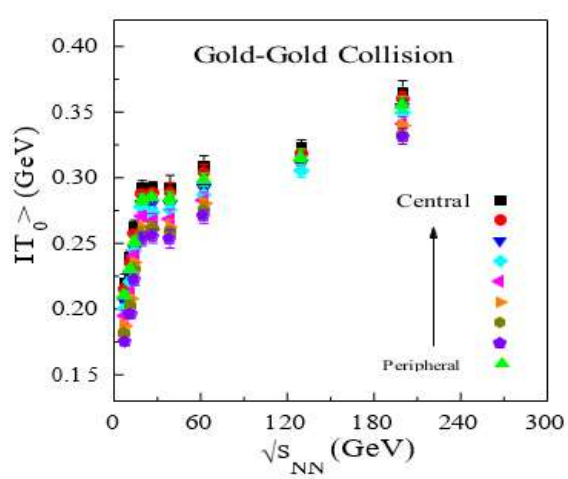

Figure 2: Dependence of average kinetic freeze-out temperature on energy and centrality

It is also reassuring that the two fitting sets (Set 1) yield essentially identical qualitative behaviours, despite minor numerical differences in a few peripheral bins. This consistency confirms that the observed dependencies are robust experimental facts rather than artefacts of the particular fitting procedure. Taken together, these intercept values paint a coherent picture of the fireball evolution: the kinetic decoupling temperature is a sensitive probe of the interplay between the initial energy density, the system size, and the stiffness of the equation of state, and the systematic shifts across the tables beautifully demonstrate how each of these factors comes into play as we change the collision centrality and the beam energy.

IV. CONCLUSIONS

In this work, we have systematically extracted the kinetic freeze-out temperature, Tkin, from the transverse momentum spectra of identified negatively charged π−, K− and p− hadrons produced in Au-Au collisions across the RHIC Beam Energy Scan, covering a broad range of centre-of-mass energies from 7.7 to 200 GeV. Our extraction procedure builds upon the effective temperatures obtained in our preceding study, from which we isolated the kinetic decoupling component by applying a linear fit to the rest-mass dependence of the effective temperature. Two independent fitting sets were employed, and their excellent qualitative agreement confirms that our results are robust and free from significant bias introduced by the particular fitting approach.

The extracted values of Tkin reveal two distinct and physically transparent trends. For a fixed collision energy, the freeze-out temperature exhibits a monotonic decline as one moves from the most central collisions toward the most peripheral ones. This centrality dependence is naturally attributed to the reduction in the system size and the corresponding decrease in the initial energy density; smaller fireballs undergo fewer rescatterings, decouple earlier, and consequently freeze out at lower temperatures. The second trend, which is equally compelling, emerges when the beam energy is varied for a fixed centrality bin. The kinetic freeze-out temperature rises steadily with increasing √sNN , but the rise is characterised by three distinct regimes. A sharp increase at the lowest energies, from 7.7 to 19.6 GeV, gives way to a pronounced plateau in the intermediate region around 19.6 to 39 GeV, which is then followed by a renewed upward climb as the system approaches the highest RHIC energies. This non-uniform energy dependence is deeply suggestive of a change in the underlying microscopic dynamics.

At low energies, the baryon-rich medium and the stiff equation of state render the system highly sensitive to the deposited energy. In the intermediate domain, the observed saturation indicates a softening of the equation of state, consistent with a transition from a hadron-dominated to a parton-dominated phase, likely in the vicinity of the QCD crossover region. At the highest energies, the system enters a well-established quark-gluon plasma phase where the extreme initial temperatures, despite the strong radial flow that cools the expanding fireball, push the decoupling surface to substantially larger values.

Beyond the immediate extraction of these temperatures, our findings carry important implications for the broader understanding of the strongly interacting medium. The observed dependencies directly constrain the transport properties of the produced matter, particularly the shear viscosity to entropy density ratio, and serve as a critical anchor for hydrodynamic simulations by specifying the exact temperature at which the fluid-dynamical description ceases to be valid and the system must be treated as a free-streaming gas. The consistency between our two fitting sets further reinforces the reliability of the Fokker–Planck approach as a viable tool for extracting freeze-out parameters from experimental data.

Overall, this study provides a comprehensive mapping of the kinetic freeze-out temperature across the RHIC energy domain and establishes it as a sensitive probe of the system size, the initial energy density, and the evolving equation of state, thereby contributing to a more complete picture of the fireball evolution from its hottest, densest stages to the final decoupling of the detected hadrons.

Data availability
All data generated or analyzed during this study are included and cited in this article.

Compliance with Ethical Standards
The authors declare that they comply with ethical standards regarding the content of this paper.

REFERENCES

1. E. Schnedermann, J. Sollfrank and U. W. Heinz, Phys. Rev. C 48, 2462-2475 (1993), doi:10.1103/PhysRevC.48.2462, [arXiv:nucl-th/9307020 [nucl-th]].
2. B. I. Abelev et al. [STAR], Phys. Rev. C 81, 024911 (2010) doi:10.1103/PhysRevC.81.024911 [arXiv:0909.4131 [nucl-ex]].
3. L. Yuan, J. N. Han, D. H. Zhang, J. Ben Slimane and Z. A. A. A. Saad, Eur. Phys. J. Plus 141, no.4, 431 (2026), doi:10.1140/epjp/s13360-026-07614-8.
4. P. P. Yang, M. Waqas, M. Ajaz, W. Xie, J. B. Slimane, H. I. Alrebdi and A. A. Haj Ismail, Eur. Phys. J. A 61, no.7, 161 (2025), doi:10.1140/epja/s10050-025-01633-2.
5. S. Prasad, doi:10.17181/ts0ew-rb520.
6. E. Braaten, K. Ingles and J. Pickett, Phys. Rev. Lett. 134, no.25, 252301 (2025) doi:10.1103/7cjr-fgdw [arXiv:2408.03935 [hep-ph]].
7. I. u. Bashir and S. Uddin, J. Exp. Theor. Phys. 124, no.3, 429-432 (2017), doi:10.1134/S1063776117030013, [arXiv:1510.08582 [hep-ph]].
8. A. Andronic, P. Braun-Munzinger and J. Stachel, Nucl. Phys. A 772, 167-199 (2006), doi:10.1016/j.nuclphysa.2006.03.012, [arXiv:nucl-th/0511071 [nucl-th]].
9. [9] A. Andronic, P. Braun-Munzinger and J. Stachel, Nucl. Phys. A 834, 237C-240C (2010) doi:10.1016/j.nuclphysa.2009.12.048 [arXiv:0911.4931 [nucl-th]].
10. J. Cleymans, H. Oeschler, K. Redlich and S. Wheaton, Phys. Rev. C 73, 034905 (2006), doi:10.1103/PhysRevC.73.034905, [arXiv:hep-ph/0511094 [hep-ph]].
11. A. Andronic, P. Braun-Munzinger and J. Stachel, Acta Phys. Polon. B 40, 1005-1012 (2009), [arXiv:0901.2909 [nucl-th]].
12. [12] M. Waqas, W. Bietenholz, K. K. Olimov, M. Ajaz, J. B. Slimane, L. A. Al-Essa and A. Haj Ismail, [arXiv:2606.26301 [hep-ph]].
13. M. Badshah, H. I. Alrebdi, M. Waqas, H. Qadir and M. Ajaz, Nucl. Phys. A 1068, 123351 (2026) doi:10.1016/j.nuclphysa.2026.123351 [arXiv:2602.03364 [hep-ph]].
14. Z. J. Yang, H. j. Xu, J. Zhao and H. Li, [arXiv:2604.20493 [nucl-th]].
15. T. Biswas, D. Dhar, S. K. Manna and P. Kumar Haldar, Braz. J. Phys. 56, no.3, 134 (2026), doi:10.1007/s13538-026-02061-3.
16. M. Waqas, F. H. Liu, J. B. Slimane, K. K. Olimov, M. Ajaz, H. I. Alrebdi and A. Haj Ismail, Annals Phys. 481, 170180 (2025), doi:10.1016/j.aop.2025.170180.
17. L. L. Li, M. Ajaz, M. Waqas, J. B. Slimane, H. I. Alrebdi and R. Guo, Mod. Phys. Lett. A 40, no.28, 2550115 (2025), doi:10.1142/S0217732325501159.
18. U. Tabassam, Y. Ali and A. Zaman, Mod. Phys. Lett. A 40, no.38, 2550195 (2025), doi:10.1142/S0217732325501950.
19. Y. Yuan, [arXiv:2509.20743 [hep-ph]].
20. J. Zhang and X. J. Wen, Universe 11, no.9, 312 (2025), doi:10.3390/universe11090312.
21. M. Waqas, M. Ajaz, T. Saidani, A. N. Tawfik and A. Haj Ismail, Eur. Phys. J. Plus 139, no.10, 934 (2024), doi:10.1140/epjp/s13360-024-05717-8.
22. D. Sahu, S. Tripathy, R. Sahoo and S. K. Tiwari, Springer Proc. Phys. 277, 369-373 (2022), doi:10.1007/978-981-19-2354-8 67.
23. K. Goswami, D. Sahu and R. Sahoo, Phys. Rev. D 107, no.1, 014003 (2023), doi:10.1103/PhysRevD.107.014003, [arXiv:2206.13786 [hep-ph]].
24. D. Sahu and R. Sahoo, J. Phys. G 48, no.12, 125104 (2021), doi:10.1088/1361-6471/ac2cd6, [arXiv:2006.04185 [hep-ph]].
25. M. Waqas, H. A. Khan, W. Bietenholz, M. Ajaz, J. B. Slimane, H. I. Alrebdi and A. Haj Ismail, Eur.

Phys. J. A 61, no.7, 156 (2025), doi:10.1140/epja/s10050-025-01626-1, [arXiv:2507.07369 [hep-ph]].

26. M. Waqas, W. Bietenholz, M. Bouzidi, M. Ajaz, A. A. Haj Ismail and T. Saidani, J. Phys. G 51, no.7, 075102 (2024), doi:10.1088/1361-6471/ad489e, [arXiv:2406.04631 [hep-ph]].
27. M. Waqas, G. X. Peng, M. Ajaz, A. A. Ismail, P. P. Yang and Z. Wazir, Universe 9,44 (2023), https://doi.org/10.3390/universe9010044, [arXiv:2112.00975 [hep-ph]].
28. M. Waqas, L. M. Liu, G. X. Peng, M. Ajaz, A. A. Haj Ismail, E. A. Dawi and A. M. Khubrani, Chin. J. Phys. 80, 206-228 (2022), doi:10.1016/j.cjph.2022.09.016.
29. S. Tang, C. Zhang, L. Zheng, R. Wan, Z. W. Lin and G. L. Ma, [arXiv:2606.28928 [nucl-th]].
30. X. Li, S. P. Wang, R. Wang, Z. Zhang, J. Pu, C. W. Ma and L. W. Chen, Phys. Rev. C 113, no.3, 034612 (2026), doi:10.1103/94s2-7yjy, [arXiv:2511.20387 [nucl-th]].
31. A. Menon Kavumpadikkal Radhakrishnan, S. Prasad, N. Mallick and R. Sahoo, J. Subatomic Part. Cosmol. 4, 100244 (2025), doi:10.1016/j.jspc.2025.100244.
32. R. Krupczak, N. Borghini and H. Roch, [arXiv:2606.22558 [nucl-th]].
33. Y. Zhang, Acta Phys. Polon. B 56, no.12, 12-A3 (2025), doi:10.5506/APhysPolB.56.12-A3.
34. M.Waqas et al., https://www.frontiersin.org/journals/physics/articles/10.3389/fphy.2026.1895766/abstract.
35. B. I. Abelev et al. [STAR], Phys. Rev. C 79, 034909 (2009) doi:10.1103/PhysRevC.79.034909 [arXiv:0808.2041 [nucl-ex]].
36. L. Adamczyk et al. [STAR], Phys. Rev. C 96, no.4, 044904 (2017) doi:10.1103/PhysRevC.96.044904 [arXiv:1701.07065 [nucl-ex]].
37. J. Adam et al. [STAR], Phys. Rev. C 101, no.2, 024905 (2020) doi:10.1103/PhysRevC.101.024905 [arXiv:1908.03585 [nucl-ex]].
38. K. Adcox et al. [PHENIX], Phys. Rev. C 69, 024904 (2004) doi:10.1103/PhysRevC.69.024904 [arXiv:nucl-ex/0307010 [nucl-ex]].
39. J. Adams et al. [STAR], Phys. Rev. Lett. 92, 112301 (2004) doi:10.1103/PhysRevLett.92.112301 [arXiv:nucl-ex/0310004 [nucl-ex]].
40. H. Zheng and L. Zhu, Adv. High Energy Phys. 2015, 180491 (2015), doi:10.1155/2015/180491, [arXiv:1510.05449 [nucl-th]].
41. Z. Xie, W. Z. Li, J. Q. Tao, H. Zheng, W. C. Zhang, W. Dai, L. L. Zhu, X. Q. Liu, D. M. Zhou and B. H. Sa, [arXiv:2606.29187 [nucl-th]].
42. S. A. Mir, S. Uddin and I. u. Bashir, Eur. Phys. J. A 62, no.3, 48 (2026), doi:10.1140/epja/s10050-026-01815-6.
43. M. Waqas, M. Ajaz, T. Saidani, A. N. Tawfik and A. Haj Ismail, Eur. Phys. J. Plus 139, no.10, 934 (2024), doi:10.1140/epjp/s13360-024-05717-8.
44. A. K. Singh, A. Akhil, S. K. Tiwari and P. Pareek, Eur. Phys. J. Plus 139, no.6, 491 (2024), doi:10.1140/epjp/s13360-024-05290-0, [arXiv:2309.17071 [nucl-th]].
45. J. Cleymans and D. Worku, Eur. Phys. J. A 48, 160 (2012) doi:10.1140/epja/i2012-12160-0 [arXiv:1203.4343 [hep-ph]].
46. M. Waqas and F. H. Liu, Eur. Phys. J. Plus 135, no.2, 147 (2020), doi:10.1140/epjp/s13360-020-00213-1, [arXiv:1911.01709 [hep-ph]].